Short Papers

A New Microstrip Dispersion Model

PRAKASH BHARTIA, SENIOR MEMBER, IEEE, AND
PROTAP PRAMANICK, STUDENT MEMBER, IEEE

Abstract—**A new unified analysis technique is presented for dispersion in microstrip at high frequencies. The technique exploits the fact that the dispersion in microstrips is due to coupling between a surface-wave mode and the LSE mode of an appropriate model of the microstrip. The analysis uses an effective dielectric constant (EDC) approach to evaluate the mode coupling in the LSE model. Unlike previously reported models, all the parameters of the model are exactly determined from the the quasistatic parameters of the microstrip, which takes the fringing field into account. Approximate closed-form equations are derived for the prediction of microstrip dispersion. The results agree within 1.50 percent with the experimental and previously published data over a wide useful range of microstrip dimensions and substrate permittivities.**

I. Introduction

Numerous papers have appeared dealing with a rigorous solution of the dispersion problem of microstrip lines. There have been highly sophisticated techniques using the spectral domain approach in conjunction with the Ritz–Galerkin method [1], [2] or the eigenmode analysis [3]. But these methods depend on time-consuming evaluation of the final relations. Moreover, these rigorous analyses fail to provide any closed-form solution useful for design purposes. As a result, there have been quite a few empirical and semi-empirical attempts at the problem, based on several hypotheses, experimental results on several materials [4], [5] and curve fitting, etc., leading to closed-form equations useful for design purposes. As far as frequency and substrate dielectric constant are concerned, each of these empirical equations has its own range of validity.

It has been reported by several authors that the surface wave plays an important role in microstrip dispersion [6], [7]. But Getsinger's model [4] does not take the effect of the surface-wave mode into account. Moreover, Getsinger's model depends upon experimental data for its complete characterization.

There have been many different approaches to the dynamic problem of microstrip characteristic impedance [8]. These approaches can be divided into two categories. In the first category, the frequency dependence of the characteristic impedance is evaluated using an equivalent parallel-plate waveguide model of the microstrip, of which all the parameters are determined empirically. Although such a model was first proposed by Kompa and Mehran [9] and the frequency dependence of the effective width of the model was experimentally verified [9], it was subsequently corrected by Owens [10]. In a later report, Owens' equation was corrected by Pues and Van de Capelle [11]. Still, it can be shown that the derivations of the equations defining the frequency-dependent effective width of the parallel-plate waveguide model and frequency-dependent characteristic impedance of the microstrip [9]–[11] are based on contradictory assumptions [12].

In the second category, microstrip characteristic impedance is calculated by solving the field problem in the spectral domain [13], which is supposed to have a very high degree of accuracy. Recently, Jansen *et al.* [14] argued for the power current formulation of microstrip characteristic impedance. This has also been supported by Getsinger [15]. According to their formulation, the characteristic impedance is evaluated as the ratio between twice the average power flowing through the microstrip to the square of the total longitudinal current. But the results obtained using Jansen's [14] and Getsinger's [15] models differ significantly.

Keeping all the above limitations of the existing theories in mind and with the intension of achieving analytical simplicity and mathematical rigor, the present work considers the dispersion in a microstrip line as a coupling between the surface-wave mode and the LSE mode of an appropriate model of the microstrip line. The parameters of the model are obtained from the static TEM parameters (characteristic impedance and effective dielectric constant) of the actual microstrip. This inherently takes the effect of fringing field into account. An EDC concept [16] is used to evaluate the mode coupling.

Although it does not completely follow from theory that the dispersion phenomena in the two structures must be identical, the validity of the model is established by the agreement of the computed results within 1.5 percent with those from existing theories and experiments.

Using the power–current definition, closed-form expressions are derived from the model for the frequency-dependent characteristic impedance and the effective width of the equivalent parallel-plate model for the microstrip.

II. Analytical Model

The conventional microstrip line structure is shown in Fig. 1(a). For the ease of analysis, this is distorted to result in the model shown in Fig. 1(b). The distorted version preserves all the quasistatic characteristics of the original microstrip, but does not have any fringing field. The effective dielectric constants ϵ_I and ϵ_{II} of Sections I and II, respectively, are obtained from y-directed resonances of the structures shown in Figs. 1(c) and (d), respectively. ϵ_I corresponds to the parallel-plate waveguide mode of the dielectric-filled portion of the model and ϵ_{II} to the lowest order surface-wave mode of the microstrip.

The parameters u and v are obtained by forcing the model to have the same electrical characteristics as the original microstrip.

Evaluation of the Dimensions of the Model

Let the static TEM parameters, effective dielectric constant and the characteristic impedance, be $\epsilon_e(0)$ and Z_0, respectively.

Manuscript received May 12, 1983; revised April 23, 1984. This research has been supported by a Natural Sciences and Engineering Research Council of Canada Grant A-0001.

P. Pramanick is with the Department of Electrical Engineering, University of Ottawa, Ottawa, Ont., Canada KIN 6N5.

P. Bhartia is with the Electronics Division, Defence Research Establishment, Ottawa, Ont., Canada K1A 0Z4.

0018-9480/84/1000-1379$01.00 ©1984 IEEE

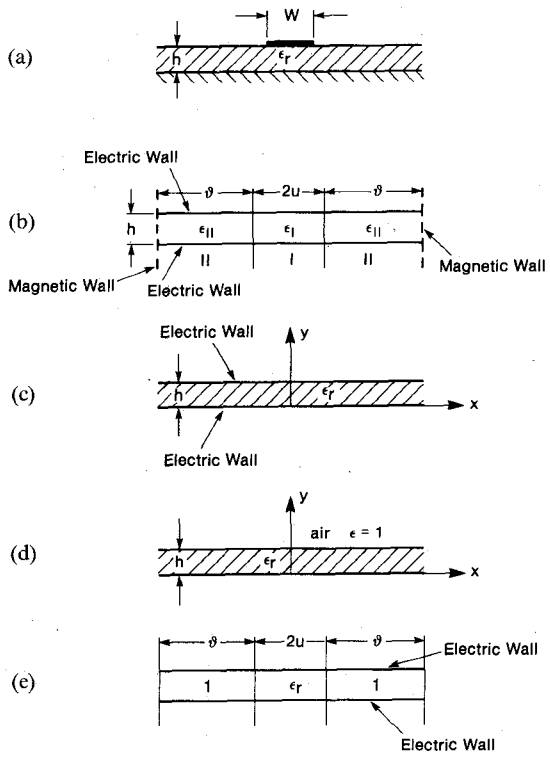

Fig. 1. (a) Microstrip line, (b) proposed equivalent model of microstrip, (c) structure for analyzing y variation in region I, (d) structure for analyzing y variation in region II, (e) equivalent model at zero frequency.

For a given W/h and ϵ_r, these parameters are computed using empirical relations [17], [18].

The per-unit-length inductance L_u and the per-unit-length capacitance C_u can be written as

$$L_u = \frac{Z_0\sqrt{\epsilon_e(0)}}{c} \tag{1}$$

and

$$C_u = \frac{\sqrt{\epsilon_e(0)}}{cZ_0} \tag{2}$$

where c is the velocity of electromagnetic wave propagation in free space.

The inductance and capacitance per unit length for the LSE model shown in Fig. 1(e) can be written as

$$L = \frac{h\mu_0}{2(u+v)} \tag{3}$$

$$C = \frac{2}{h}(\epsilon_r u + v)\epsilon_0 \tag{4}$$

where μ_0 and ϵ_0 are the permeability and permittivity of free space, respectively.

On equating the equivalent parameters

$$u = \frac{\eta_0 h}{2Z_0(\epsilon_r - 1)}\left(\sqrt{\epsilon_e(0)} - \frac{1}{\sqrt{\epsilon_e(0)}}\right) \tag{5}$$

where η_0 is the free-space wave impedance $= 120\pi\ \Omega$

$$v = \frac{\eta_0 h}{2Z_0(\epsilon_r - 1)}\left(\frac{\epsilon_r}{\sqrt{\epsilon_e(0)}} - \sqrt{\epsilon_e(0)}\right). \tag{6}$$

The dielectric filling factor is given by

$$q = \frac{uh}{uh + vh} = \frac{u}{u+v}. \tag{7}$$

Using (5) and (6) gives

$$q = \frac{\epsilon_e(0) - 1}{\epsilon_r - 1}. \tag{8}$$

Equation (8) gives the same filling factor as the original microstrip, which is not the case in Getsinger's model [4].

Effective Dielectric Constants ϵ_I and ϵ_{II} from y-Directed Resonances

a) Evaluation of ϵ_I: Considering Fig. 1(c), the y-directed resonance gives

$$(1/\gamma_y)\tanh(\gamma_y h) = 0 \tag{9a}$$

where γ_y is the y-directed wavenumber. The solutions for (9) are a function of the frequency and the substrate height h. For a lossless ground plane and strip and $2\sqrt{\epsilon_r}h < \lambda_0$, which is the case for the general frequency range of microstrip operation

$$\gamma_y = 0. \tag{9b}$$

Since

$$\epsilon_I = \epsilon_r + \frac{\gamma_y^2}{k_0^2} \tag{10}$$

it follows that, for the above-mentioned condition

$$\epsilon_I = \epsilon_r. \tag{11}$$

b) Evaluation of ϵ_{II}: The quantity of ϵ_{II} can be derived by solving the eigenvalue equation of the layered structure shown in Fig. 1(d). For such a structure

$$E_y = \frac{1}{\epsilon_r(y)}\left(k_z^2 - \frac{\partial^2}{\partial x^2}\right)\phi_e(y) \tag{12}$$

where

$$\phi_e(y) = \cosh(\gamma_y y), \qquad 0 < y \leqslant h \tag{13}$$

and

$$\phi_e(y) = A_y \exp\left[-\gamma_{y0}(y-h)\right], \qquad h \leqslant y < \infty \tag{14}$$

k_z is the z-directed propagation constant.

Matching the field components E_z and H_x at $y = h$, we obtain

$$\frac{\gamma_y}{\epsilon_r}\sinh(\gamma_y h) + \gamma_{y0}\cosh(\gamma_y h) = 0. \tag{15}$$

The phase constants γ_y and γ_{y0} are related via

$$\gamma_{y0}^2 = (\epsilon_r - 1)k_0^2 + \gamma_y^2 \tag{16}$$

where k_0 is the free-space propagation constant. The solutions of (15) and (16) yield γ_y and the effective dielectric constant ϵ_{II} of region II is given by

$$\epsilon_{II} = \epsilon_r + \left(\frac{\gamma_y}{k_0}\right)^2. \tag{17}$$

Therefore, we notice from (17) that ϵ_{II} is a function of frequency.

LSE Model

Up to this point of the analysis, we have completely defined the different parameters of the LSE model. The electric and

magnetic fields for this model can be written as:

$$\left.\begin{aligned} H_{zu} &= A_u \sinh(\gamma_u x) && (18)\\ E_{yu} &= \frac{j\omega\mu_0}{\gamma_u} A_u \cosh(\gamma_u x) && (19)\\ H_{xu} &= -\left(\frac{\gamma}{\gamma_u}\right) A_u \cosh(\gamma_u x) && (20)\end{aligned}\right\} \quad 0 \leqslant x < u$$

$$\left.\begin{aligned} H_{zv} &= A_v \sinh(\gamma_v(u+v-x)) && (21)\\ E_{yv} &= \frac{j\omega\mu_0}{\gamma_v} A_v \cosh(\gamma_v(u+v-x)) && (22)\\ H_{xv} &= -\left(\frac{\gamma}{\gamma_v}\right) A_v \cosh(\gamma_v(u+v-x)) && (23)\end{aligned}\right\} \quad u \leqslant x \leqslant u+v.$$

The propagation constants are related by

$$\gamma_u^2 + \gamma_z^2 + \epsilon_{\mathrm{I}} k_0^2 = 0 \tag{24}$$

in region I and by

$$\gamma_v^2 + \gamma_z^2 + \epsilon_{\mathrm{II}} k_0^2 = 0 \tag{25}$$

in region II. In (24) and (25), γ_z is the propagation constant in the z-direction, which applies to both regions I and II.

In order for the H_z and E_y fields to be continuous at the interface between the two regions I and II, the following conditions are imposed on (18) through (23):

$$A_u \sinh(\gamma_u u) = A_v \sinh(\gamma_v v) \tag{26}$$

$$\frac{A_u}{\gamma_u}\cosh(\gamma_u u) = \frac{A_v}{\gamma_v}\cosh(\gamma_v v). \tag{27}$$

Dividing (26) by (27), the following transcendental equation is obtained

$$\gamma_u \tanh(\gamma_u u) + \gamma_v \tanh(\gamma_v v) = 0 \tag{28}$$

which together with the relation

$$\gamma_v^2 = (\epsilon_{\mathrm{I}} - \epsilon_{\mathrm{II}}) k_0^2 + \gamma_u^2 \tag{29}$$

derivable from (24) and (25), determines the solution for the wavenumbers γ_u and γ_v. Once γ_u and γ_v are obtained, the frequency-dependent effective dielectric constant of the microstrip is given by

$$\epsilon_e(f) = \epsilon_{\mathrm{I}} + \frac{\gamma_u^2}{k_0^2} = \epsilon_{\mathrm{II}} + \frac{\gamma_v^2}{k_0^2}. \tag{30}$$

Equation (28) has the same form as [4, eq. (8)]; however, it does not contain any unknown parameter as [4, eq. (8)] does.

Closed-Form Solution

If the approximation

$$\tanh\theta = \left[\frac{1}{\theta} + \frac{\theta}{3}\right]^{-1} \tag{31}$$

is made in (15), it gives the equation

$$\gamma_y^6 + a_2\gamma_y^4 + a_1\gamma_y + a_0 = 0 \tag{32}$$

$$a_2 = (2p + qp^2 - r)/p^2 \tag{33}$$

$$a_1 = (2pq + 1)/p^2 \tag{34}$$

$$a_0 = q/p^2 \tag{35}$$

where

$$p = h/3 \tag{35a}$$

$$q = (\epsilon_r - 1)k_0^2 \tag{35b}$$

$$r = (h/\epsilon_r)^2. \tag{35c}$$

The error in (31) is less than 0.75 percent for $\theta \leqslant 0.8$.

Solving (32) and using (17) gives

$$\epsilon_{\mathrm{II}} = \epsilon_r + (s_1 + s_2 - a_2/3)/k_0^2 \tag{36}$$

where

$$s_1 = \left[\eta_2 + \left(\eta_1^3 + \eta_2^2\right)^{1/2}\right]^{1/3} \tag{37a}$$

$$s_2 = \left[\eta_2 - \left(\eta_1^3 + \eta_2^2\right)^{1/2}\right]^{1/3} \tag{37b}$$

and

$$\eta_1 = a_1/3 - a_2^2/9 \tag{38}$$

$$\eta_2 = (a_1 a_2 - 3a_0)/6 - a_2^3/27. \tag{39}$$

In general, the approximation (31) is valid within the highest frequency range of microstrip operation which is the cutoff frequency of TE_1 mode and given by

$$f_{\mathrm{CTE}_1} = \frac{c}{4h\sqrt{\epsilon_r - 1}}. \tag{40}$$

Using the same approximation of (31), (28) gives

$$(\epsilon_r - \epsilon_e(f))^2 - \left(\frac{3}{uvk_0^2} + (\epsilon_r - \epsilon_{\mathrm{II}})\right)(\epsilon_r - \epsilon_e(f)) + \frac{3(\epsilon_r - \epsilon_{\mathrm{II}})}{u(u+v)} = 0 \tag{41}$$

and solving (41) gives

$$\epsilon_e(f) = \epsilon_r - \left(\epsilon_r - \epsilon_{\mathrm{II}} + \frac{3}{uvk_0^2}\right) \cdot \left[1 - \left\{1 - \frac{\frac{12(\epsilon_r - \epsilon_{\mathrm{II}})}{u(u+v)}}{\left(\epsilon_r - \epsilon_{\mathrm{II}} - \frac{3}{uvk_0^2}\right)^2}\right\}^{1/2}\right]. \tag{42}$$

Expanding the square root binomially up to the second term and using (5) and (6) gives

$$\epsilon_e(f) = \epsilon_r - \frac{K_1(\epsilon_r - \epsilon_e(0))}{1 + K_2(f/f_p)^2} \tag{43}$$

where

$$f_p = \frac{Z_0}{2\mu_0 h} \tag{44}$$

$$K_1 = \frac{\epsilon_r - \epsilon_{\mathrm{II}}}{\epsilon_r - 1} \tag{45}$$

$$K_2 = \frac{\pi^2}{12}\frac{(\epsilon_r - \epsilon_e(0))(\epsilon_e(0) - 1)(\epsilon_r - \epsilon_{\mathrm{II}})}{(\epsilon_r - 1)^2 \epsilon_e(0)}. \tag{46}$$

A study of (43) shows that the frequency dependence of $\epsilon_e(f)$ is asymptotic at zero and infinite frequencies and $\epsilon_e(f)$ goes from a value of $\epsilon_e(0)$ at zero frequency to ϵ_r at infinite frequency, in agreement with theory [19].

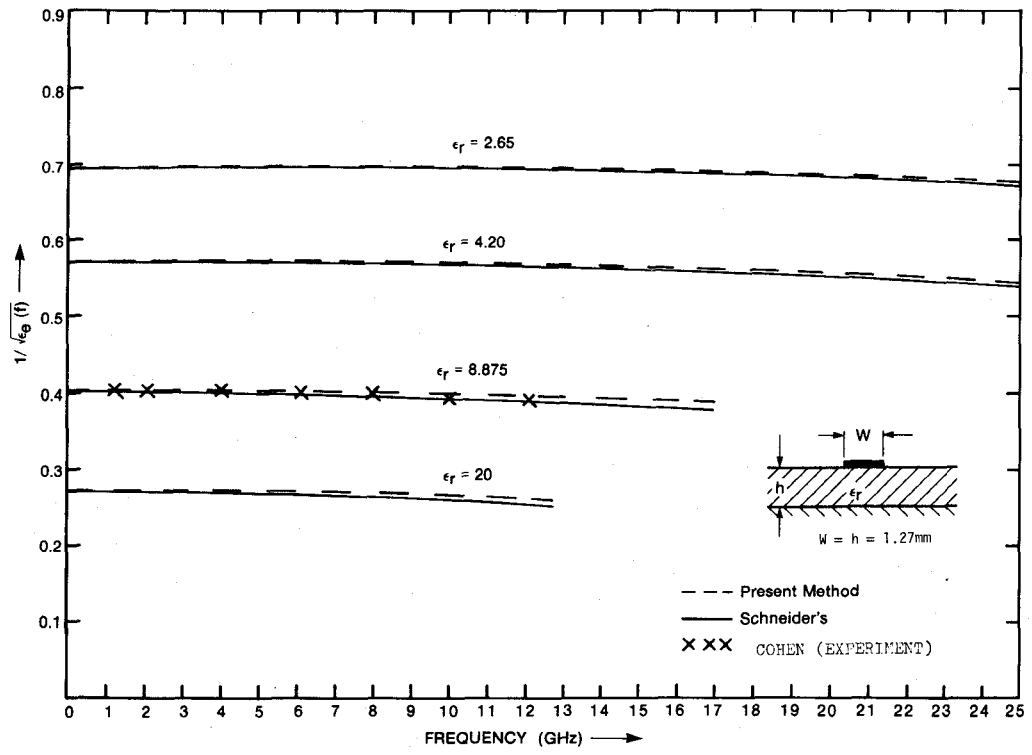

Fig. 2. Microstrip dispersion for standard open microstrip transmission line for $w = h = 1.27$ mm. $1/\sqrt{\epsilon_e(f)}$ plotted as a function of frequency for $\epsilon_r = 2.65$, 4.20, 8.875, and 20.00.

III. Characteristic Impedance

Knowing the modal field expressions from (18) through (23), it is possible to compute the frequency-dependent characteristic impedance of the microstrip. For reasons outlined above, we assume the following definition:

$$Z_0(f) = \frac{2P}{I_z^2} \tag{47}$$

where P is the total average power flowing through the microstrip and I_z is the total longitudinal current. Computing P and I_z from (18) through (23) results in the frequency-dependent characteristic impedance

$$Z_0(f) = \frac{\eta_0 h}{W_e(f)\sqrt{\epsilon_e(f)}} \tag{48}$$

where $W_e(f)$, the frequency-dependent effective width of the equivalent parallel plate waveguide model for the microstrip, is given by

$$W_e(f) = \frac{2\left[\left\{\frac{\sinh(2\gamma_u u)}{4\gamma_u} + \frac{u}{2}\right\} + \left\{\frac{\cosh(\gamma_u u)}{\cosh(\gamma_v v)}\right\}^2 \left\{\frac{\sinh(2\gamma_v v)}{4\gamma_v} + \frac{v}{2}\right\}\right]^{-1}}{\left[\frac{\sinh(\gamma_u u)}{\gamma_u} + \left\{\frac{\cosh(\gamma_u u)}{\cosh(\gamma_v v)}\right\}\frac{\sinh(\gamma_v v)}{\gamma_v}\right]^{-2}} \tag{49}$$

The right-hand side of (49) converges to $W_e(0)$, the static TEM effective width, as the frequency approaches zero.

IV. Comparison with Other Theories and Measurements

The theory developed in the present work is compared with the experimental results of Cohen [20] and the theory developed by Schneider [6]. This is shown in Fig. 2 for open microstrip lines with $W = h = 1.27$ mm and $\epsilon_r = 2.65$, 4.20, 8.875, and 20.00. It can be observed that the present theory is closer to the experimental data of Cohen [20], which agrees accurately with the full-wave theory of Mittra and Itoh [21].

A second comparison of the present theory with other theories and experimental data is shown in Fig. 3, for $W/h > 1$ and $\epsilon_r = 10.1$. Curve 2 is due to Edwards and Owens [5] and is obtained from curve fitting to experimental data. Curve 1 is due to Schneider [6] and the present theory. The maximum deviation between the curves is less than 1.50 percent.

The last comparison of the present theory with experiment is shown in Fig. 4 for $W/h < 1$. The experimental points are due to Denlinger [19]. Fig. 4 shows that the present theory has better agreement than Schneider's [6] theory with the experimental results.

The computed results for $Z_0(f)$ as a function of frequency using the present model are shown in Fig. 5 and compared with Getsinger's analytical and experimental results [15], for $h = 6.35$ mm and $W = 2.54$, 6.35, and 12.70 mm on alumina substrate of $\epsilon_r = 9.74$. The static TEM parameters of the microstrip were calculated using Hammerstad and Jensen's [22] highly accurate formulas for microstrip. Although Getsinger's LSE model agrees reasonably with his experimental results, the discrepancy between the present model and Getsinger's model is due to the error in the computation of static TEM parameters in his model. For example, the characteristic impedance of the microstrip with $W = 2.54$

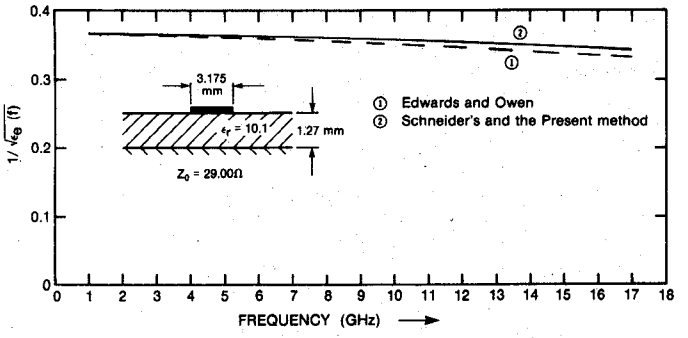

Fig. 3. Microstrip dispersion for open microstrip transmission line for $w/h = 2.5$, $\epsilon_r = 10.1$, $Z_0 = 29.00\ \Omega$.

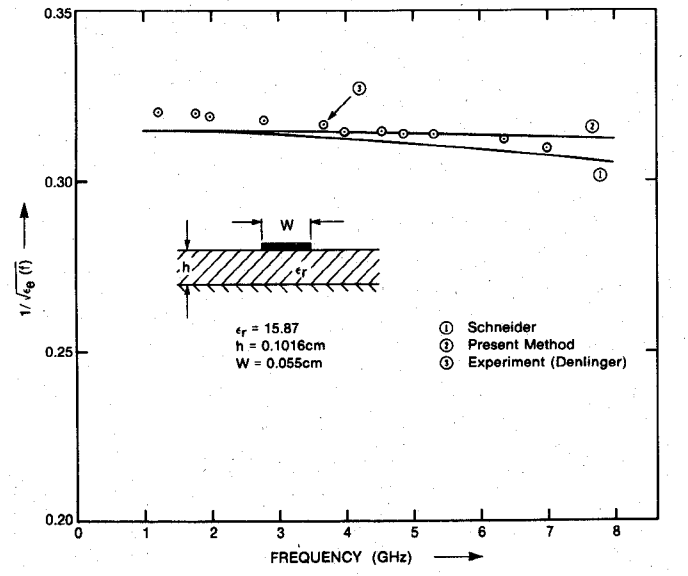

Fig. 4. Microstrip dispersion for open microstrip transmission line for $w/h = 0.54134$, $Z_0 = 51.6\ \Omega$.

mm, $h = 6.35$ mm, and $\epsilon_r = 9.74$ is 72.50 Ω. But in Getsinger's work [15], it is shown to be 70 Ω. Moreover, in the present model $Z_0(f)$ increases very slowly with frequency as predicted by Bianco *et al.* using two other models [23]. Besides making many other approximations, Getsinger's model does not include the modal coupling. In the present model, coupling with a surface-wave mode is taken into consideration using an effective dielectric constant approach. Since the effect of a surface wave is more pronounced for high-impedance lines, the discrepancy between Getsinger's and the present model reduces for low-impedance lines as observed in Fig. 5. Therefore, it is believed that the present model will give better results.

V. Conclusions

In the preceding sections, dispersion in the open microstrip line has been analyzed using the effective dielectric constant concept to evaluate the coupling between a spurious surface-wave mode of the microstrip and the LSE mode in an appropriate model of the microstrip which preserves all the quasistatic characteristics of the microstrip. The results obtained by using this theory agree within 1.5 percent with other empirical and semi-empirical theories. Although the method has been verified for $2.65 \leqslant \epsilon_r \leqslant 20$, $0.54 \leqslant W/h \leqslant 2.5$ it is expected to be valid outside these ranges, because the model is quite general.

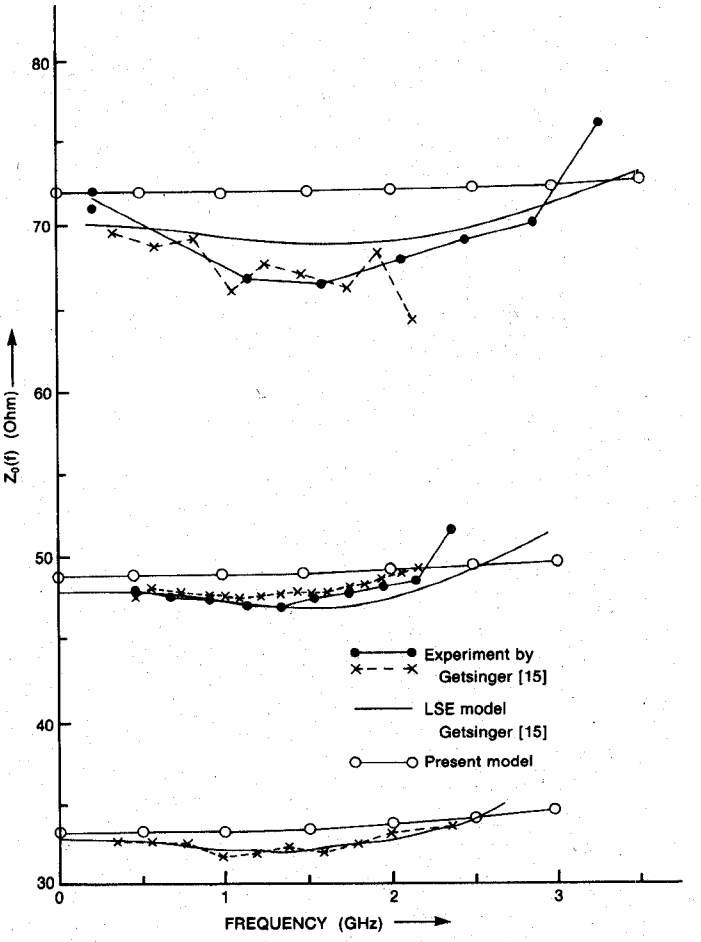

Fig. 5. Variation of characteristic impedance with frequency for open microstrip $w = 2.54$, 6.35, and 12.70 mm, $h = 6.35$ mm, $\epsilon_r = 9.74$.

Since, in determining the mode coupling, only the lowest order surface-wave mode has been considered, the present equations will be valid up to the onset of the TE_1 surface-wave mode, which is the highest frequency limit for microstrip operation. The accuracy of the method can be improved by computing the quasistatic parameters more accurately.

Using small argument approximations of certain transcendental functions, closed-form equations are derived. These may be useful for many design purposes. None of these equations require any empirical constants to be derived from experimental results or curve fitting.

Assuming a power–current relationship, an expression for the frequency-dependent characteristic impedance has been found that fits the other theories which assume the same definition for the characteristic impedance. In addition, the derived expression for the frequency-dependent effective width of the equivalent parallel-plate waveguide will be useful in analyzing microstrip discontinuities and evaluating microstrip power handling capability.

References

[1] T. Itoh, "Generalized spectral-domain method for multiconductor printed lines and its application to tunable suspended microstrips," *IEEE Trans. Microwave Theory Tech.*, vol. MTT-26, pp. 983–987, Dec. 1978.

[2] T. Itoh and R. Mittra, "Spectral-domain approach for calculating dispersion characteristics of microstrip lines," *IEEE Trans. Microwave Theory Tech.*, vol. MTT-21, pp. 496–498, June 1973.

[3] A. K. Saad and K. Schunemann, "Efficient eigenmode analysis for

planar transmission lines," *IEEE Trans. Microwave Theory Tech.*, vol. MTT-30, pp. 2125–2131, Dec. 1982.
[4] W. J. Getsinger, "Microstrip dispersion model," *IEEE Trans. Microwave Theory Tech.*, vol. MTT-21, pp. 34–39, Jan. 1973.
[5] T. C. Edwards and R. P. Owens, "2-18 GHz dispersion measurements on 10-100 ohm microstrip lines on sapphire," *IEEE Trans. Microwave Theory Tech.*, vol. MTT-24, pp. 506–513, Aug. 1976.
[6] M. V. Schneider, "Microstrip dispersion," *Proc. IEEE*, vol. 60, pp. 144–146, Jan. 1972.
[7] M. Kobayashi, "Important role of inflection frequency in the dispersive property of microstrip lines," *IEEE Trans. Microwave Theory Tech.*, vol. MTT-30, pp. 2057–2059, Nov. 1982.
[8] K. C. Gupta, R. Garg, and I. J. Bahl, *Microstrip Lines and Slotlines*. Dedham, MA: Artech House, 1979, p. 91.
[9] G. Kompa and R. Mehran, "Planar waveguide model for calculating microstrip components," *Electron. Lett.*, vol. 11, pp. 459–460, 1975.
[10] R. P. Owens, "Predicted frequency dependence of microstrip characteristic impedance using the planar wave-guide model," *Electron. Lett*, vol. 12, pp. 269–270, 1976.
[11] H. F. Pues and A. R. van de Capelle, "Approximate formulas for frequency dependence of microstrip parameters," *Electron. Lett.*, vol. 16, no. 23, pp. 870–872, 1980.
[12] P. Pramanick and P. Bhartia, "Frequency dependence of effective width of planar waveguide model for microstrips," submitted for publication.
[13] J. B. Knorr and A. Tufekcioglu, "Spectral-domain calculation of microstrip characteristic impedance," *IEEE Trans. Microwave Theory Tech.*, vol. MTT-23, pp. 725–728, 1975.
[14] R. H. Jansen and M. Kirsching, "Arguments and an accurate model for the power current formulation of microstrip characteristic impedance," *Arch. Elek. Ubertragung*, vol. 37, pp. 108–112, 1983.
[15] W. J. Getsinger, "Measurement and modelling of apparent characteristic impedance of microstrip," *IEEE Trans. Microwave Theory Tech.*, vol. MTT-31, pp. 624–632, Aug. 1983.
[16] R. M. Knox and P. P. Toulios, "Integrated circuits for the millimeter through optical frequency range," in *Proc. Symp. on Submillimeter Waves*. Brooklyn, NY, Polytechnic Press of Polytechnic Inst., 1976, pp. 497–516.
[17] H. A. Wheeler, "Transmission line properties of parallel strips separated by a dielectric sheet," *IEEE Trans. Microwave Theory Tech.*, vol. MTT-23, pp. 280–289, Mar. 1964.
[18] M. V. Schneider, "Microstrip lines for microwave integrated circuits," *Bell Syst. Tech. J.*, vol. 48, no. 3, pp. 1421–1444, 1969.
[19] E. J. Denlinger, "A frequency dependent solution for microstrip transmission lines," *IEEE Trans. Microwave Theory Tech.*, vol. MTT-19, pp. 30–39, Jan. 1971.
[20] R. Mittra and T. Itoh, *Advances in Microwaves*. New York: Academic, 1974.
[21] R. Mittra and T. Itoh, "A new technique for the analysis of the dispersion characteristics in microstrip lines," *IEEE Trans. Microwave Theory Tech.*, vol. MTT-19, pp. 47–56, Jan. 1971.
[22] E O. Hammerstad and Ø. Jensen, "Accurate models for microstrip computer aided design," in *IEEE MTT-S Int. Microwave Symp. Dig.*, 1980, pp. 407–409.
[23] B. Bianco, L. Panini, M. Parodi, and S. Ridella, "Some considerations about the frequency dependence of the characteristic impedance of uniform microstrips," *IEEE Trans. Microwave Theory Tech.*, vol. MTT-26, pp. 182–185, Mar. 1978.

Microwave Point Contact Diode Responsivity Improvement through Surface Effects in Vacuum

N. S. KOPEIKA, SENIOR MEMBER, IEEE, ISRAEL HIRSH, AND M. RAVFOGEL

***Abstract*—Desorption of air atoms from point contact diode surfaces via exposure to vacuum can give rise to significant changes in electronic characteristics. In the example considered, exposure of an *X*-band detector to a modest vacuum gives rise to a responsivity increase of about 80 percent for video and heterodyne detection. Experiments indicate that vacuum desorption of minority surface impurities increases the barrier height and decreases tunneling probability, thus increasing diode nonlinearity and making the diodes more nearly "ideal." The resulting relative increase of the thermionic emission current should decrease the effective shot-noise temperature, thus increasing the signal-to-noise ratio (SNR) even further.**

Manuscript received January 4, 1984; revised May 10, 1984.

The authors are with the Department of Electrical and Computer Engineering, Ben-Gurion University of the Negev, Beer-Sheva, Israel 84120.

I. Introduction

Recent experiments with light emitting diodes (LED's) [1] and photodiodes [2] have indicated that, despite "hermetic sealing," immersion of such devices in even modest vacuums for several hours or even days gives rise to desorption of surface-adsorbed gases from passivation layers and to subsequent semiconductor free charge carrier diffusion and redistribution which significantly alter diode electronic and optical properties. Changes in the current–voltage ($I-V$) and capacitance–voltage ($C-V$) characteristics reflect the loss in charge which previously had been contributed by adsorbed gas atoms that had now been desorbed. Resulting free charge redistribution can alter significantly the effective junction depletion layer width both at the surface and in the bulk. For surface-emitting LED's, these can involve significant wavelength tuning through changes in surface bandbending [1], [2]. For photodiodes, significant quantum efficiency improvement is obtainable as a result of reduced surface recombination [3]. In view of such significant alterations in p-n optoelectronic diode properties under vacuum, a preliminary investigation was launched as to effects of vacuum on electronic and microwave detection properties of point contact diodes. In the latter, the metal–semiconductor surface is much more exposed than in evaporated metal Schottky barrier devices. The experimental results indicate significant changes in point contact diode electronic properties have indeed occurred. In vacuums on the order of only 0.05 torr, microwave responsivity is on the order of 80 percent greater than that in the open air, for both video and heterodyne detection.

II. Experiments

The diodes used in these experiments were *thermocompression bonded* IN23C point contact cartridge mixer *X*-band detectors manufactured by Microwave Associates, Inc. (The choice was based entirely on convenience—these were available in quantity in our facility.) Like the diodes of [1]–[3], they are *supposed to be* "hermetically sealed." Nevertheless, these point contact diodes *also* exhibited significant changes resulting from prolonged exposure to vacuum conditions. Since internal fabrication details are unknown to us, this work will concentrate on *changes* in diode parameters brought about by a vacuum environment, rather than on the actual parameters themselves. The diodes were placed in a 3-cm-diameter cylindrical experimental metal cell attached to a vacuum system, described in detail in [1]. Diode length was aligned parallel to the incident RF electric field. Closing this cell was a glass window of 2-cm diameter through which the *X*-band radiation could propagate into the cell. The aperture diameter was sufficiently large so as to permit propagation through it at these wavelengths. All experiments, including those at atmospheric pressure air, took place with the diodes in the experimental cell. The only difference in the experiments was the air pressure within the cell.

Forward and reverse $I-V$ characteristics are compared at atmospheric pressure air and under vacuum conditions in Figs. 1 and 2. Although reverse-bias conductivity decreases in vacuum, the opposite is true under forward-bias conditions. Since device

0018-9480/84/1000-1384$01.00 ©1984 IEEE